Original Research

SOS1 promotes epithelial-mesenchymal transition of Epithelial Ovarian Cancer(EOC) cells through AKT independent NF-κB signaling pathway

Min Cheng [a,1], Xiaolin Ye [b], Jiemin Dai [b], Feiji Sun [c,*]

[a] Department of Reproductive Medicine Centre, Affiliated Hospital of Zunyi Medical University, Zunyi City, 563000, Guizhou Province, P.R. China
[b] Department of Obstetrics and Gynecology, First Affiliated Hospital of Chongqing Medical University, Chongqing 400016, P.R. China
[c] Department of Neurosurgery, Affiliated Hospital of Zunyi Medical University, Zunyi City, 563000, Guizhou Province, P.R. China

ABSTRACT

We aimed to explore the role and mechanism of SOS1 (Son of sevenless homolog 1) in malignant behaviors of epithelial ovarian cancer (EOC) cells Hey with high metastatic potential. Firstly, compared with Hey-WT (wild type) and Hey-NT (none targeted) cells, Hey-SOS1i cells showed decreased polarities, disorders in cytoskeleton arrangement. Numbers of transwell migrated, invaded, intravasation cells and extravasated cells were decreased significantly. Hey-NT cells and Hey-SOS1i cells were employed to establish a peritoneal dissemination model in nude mice. Hey-SOS1i cells formed less implantation metastatic foci in the abdominal cavity than Hey-NT cells, especially on the intestine and diaphragm in the 5th week after the tumor cells were injected intraperitoneally. SOS1 knockdown in Hey cells resulted in increased E-cadherin and decreased Vimentin, N-cadherin, MMP2, and MMP9, together with reduced Snail and activation of NF-κB pathway. Together, these results suggest SOS1 might induce EMT through activating AKT independent NF-κB pathway and the transcriptive activity of Snail, and subsequently regulate the cytoskeleton reprogramming and cell motility of Hey, one of EOC cells with high metastatic potential. This may provide some new targets for the treatment of ovarian cancer with high metastatic potential.

Introduction

Ovarian cancer is the most lethal gynecological cancer in the world for lack of an effective earlier screening measure the high mortality of ovarian tumor, which is largely explained by the fact that the majority (75%) of patients have been found at an advanced stage with widely metastatic sites in the peritoneal cavity [1]. Although in recent clinical therapy, cytoreductive surgery with adjunctive chemotherapy can improve the prognosis of ovarian cancer, most of the patients still relapse within 1 to 2 years and the 5-year overall survival rate is about 30% ∼ 40%. Therefore, the current key is to explore the invasion mechanism of epithelial ovarian cancer (EOC) and reduce the metastases of ovarian cancer by a targeted intervention.

Ovarian carcinoma tumorigenesis either progresses along a stepwise mutation process from a slow-growing borderline tumor to a well-differentiated carcinoma (type I) or involves a genetically unstable high-grade serous carcinoma that metastasizes rapidly and extensively (type II) [2]. The metastatic process consists of a series of steps [3], all of which must be completed to give rise to a metastatic tumor. The process of metastases has been divided into 4 steps. (1) Tumor cells have lost cell-cell adhesion and invaded the adjacent tissues. (2) Tumor cells might get into the blood circulatory system indirectly via the lymphatic system and maintain alive. (3) The cells might then extravasate from the circulation into the surrounding tissue. (4) Once in the new site, cells must initiate and maintain growth to form pre-angiogenic micro-metastases. However, recent data show that the number of circulating tumor cells (CTCs) in the peripheral circulation is directly related to the prognosis of epithelial ovarian cancer, indirectly suggesting that the invasion and metastasis of EOC still follow the above four steps [4].

Epithelial-mesenchymal transition(EMT) has been deemed to be related to tumor invasion and metastases via increasing Vimentin, fibronectin, N-cadherin, MMP2, and MMP9. The process of EMT is regulated by Zinc Finger Protein family, containing Snail, Slug, Twist, ZEB1, and ZEB2 [5-7].

Ras superfamily is divided into five principal families: Ras, Rho, Rab, Arf, and Ran families. Ras family combined with receptors, participate in

and adjust multiple signaling pathways, which control cell proliferation, differentiation, aging, and death. Meanwhile, it has the interaction function with Rho family in regulating cell migration and invasion [8, 9]. Guanine nucleotide exchange factors (GEFs) catalyze the release of GDP, allowing GTP to bind. In their active, GTP-bound state, Ras, and Rho GTPases interact with target proteins to promote a cellular response [10].

SOS 1 is a member of SOS family, which is the GEFs of Ras family. Stimulation of cells with growth factors leads to the association of SOS-Grb2 complexes with activated receptors and then to the stimulation of Ras through the juxtaposition of SOS and Ras at the membrane [11, 12]. A previous study showed that SOS1 promotes metastasis in ovarian cancer [13]. It is established that SOS1 is important for the tumorigenesis and progress of tumors through the activation of Ras or Rac. Furthermore, SOS1 is a functional component of the pathway connecting EGFR to NF-κB activation and the guanine nucleotide exchange activity of SOS1 is not required for NF-κB activation [12]. Activated NF-κB directly acts on the main switch of EMT, snail-related zinc finger protein transcription factors, such as Snail [14] Slug [15], ZEB1, and ZEB2 [16, 17], which regulate the expression of E-cadherin and EMT process.

Although the role of Ras activation in EMT has been reported in the literature [18], the influence and regulation of SOS1 on EMT of tumor cells is rarely mentioned in the literature. In the present experiment, we first screened out the mesenchymal-like Hey cells with high motility potential. After silencing the expression of SOS1 by lentivirus technology, we detected the changes of cell migration, invasion, and EMT-related phenotype, and investigated the underlying mechanism.

Materials and Methods

Patient samples

A total of 31 epithelial ovarian cancer (EOC) samples were collected from the Department of Gynecology of the First Affiliated Hospital of Chongqing Medical University (Chongqing, China), between May 2017 and December 2019. The tissue samples were obtained from patients who had undergone primary cytoreductive surgery. Additionally, 19 with benign ovarian tumor and 14 normal ovarian tissue samples were enrolled as control.

Cell line, lentiviral and adenovirus production, and infection

Human ovarian serous papillary ovarian cancer, Hey, was provided from Shanghai Genechem Company (Shanghai, China; bought from ATCC). SKOV3, ES-2, 3AO, and OVCAR3 cells were obtained from the Department of Pathology, Chongqing Medical University (Chongqing, China). Cells were maintained in RPMI1640 supplemented with 10% FBS, 1% penicillin, and 1% streptomycin at 37 °C and 5% CO2.

For RNA interfering, small interfering RNAs (siRNAs) (Genechem, Shanghai, China) targeting SOS1 and control siRNAs were transfected into Hey cells by Lentiviral vectors. The sequences of the two SOS1 siRNA targeting constructs were as follows: 5′-CACAGTTGAGTGGCA-TATA-3′ (SOS1i-#1) and 5′-GTGCTGACAAGGTATTGATGGA-3′(SOS1i-#2). The non-target shRNA sequence was as follows: 5′-CAACAA-GATGAAGAGCACCAA-3′. The specific adenovirus vectors overexpression SOS1 and the Negative non-targeting control adenovirus were constructed by Shanghai GeneChem Co. Ltd. (Shanghai, China). The sequences of the SOS1 constructs were as follows: 5′- GGACCTC-TATCTCAGACCCT -3′. Virus-containing Hey cells were established according to the protocol. The SOS1 knockdown cells and control cells were established using G418 screening and are referred to as SOS1i#1 or SOS1i#2 and NT.cont cells, respectively.

Western blot analysis

Hey and OVCAR3 cells treated under various conditions were washed with cold PBS and suspended for 30 min in 0.4 ml of a hypotonic lysis buffer (20 mM Tris–HCl (pH 7.5), 10 mM NaCl, 1 mM EDTA, 2 mM Na3VO4,) containing protease inhibitors (10 μg/ml leupeptin, 1 μm pepstatin). The cells were then lysed with 12.5 μl of 10% nonyl phenoxylpolyethoxylethanol (NP-40). The homogenate was centrifuged, and the supernatant, which contained the cytoplasmic extracts, was stored at −80°C. The nuclear pellet was resuspended in 25 μl of ice-cold nuclear-extraction buffer for 30 min, with intermittent mixing. Then, the extract was centrifuged, and the supernatant containing the nuclear extract was obtained. The protein content was measured by using the BCA protein assay kit (Pierce, Rockford, IL, USA). The nuclear and cytoplasmic extracts (40 μg of protein) were washed with cold PBS and suspended for 30 min in 0.4 ml of a hypotonic lysis buffer containing protease inhibitors. All cells were then lysed with 12.5μl of 10% nonyl NP-40. The homogenate was centrifuged, and the supernatant, which contained the cytoplasmic extracts, was stored at -80°C. The nuclear pellet was resuspended in 25μl of ice-cold nuclear-extraction buffer for 30 min, with intermittent mixing. Then, the extract was centrifuged, and the supernatant containing the nuclear extract was obtained. The protein content was measured by using the BCA protein assay kit (Pierce, Rockford, IL, USA). The proteins in the lysates (40μg) were separated by SDS-PAGE and transferred onto polyvinylidenedifluoride (PVDF) membrane (Millipore, Billerica, MA, USA). After blocking with 5% nonfat milk in PBST, the primary antibodies for SOS1(Sigma, 1:1000), Ras (Sigma, 1:1000), Ras-GTP(Sigma, 1:500), Rac(Sigma, 1:500), Rac-GTP (Sigma, 1:500), p-PI3K((Cell Signaling Technology, 1:500), PI3K(Cell Signaling Technology, 1:1000), p-AKT(Cell Signaling Technology, 1:500), AKT(Cell Signaling Technology, 1:500), p-ERK(Cell Signaling Technology, 1:1000), ERK(Cell Signaling Technology, 1:1000), p38MAPK(Cell Signaling Technology, 1:800), p-p38MAPK Cell Signaling Technology, 1:800), p-JNK Cell Signaling Technology, 1:500), JNK(Cell Signaling Technology, 1:500), NF-κB P65(Cell Signaling Technology 1:500), IκB(Cell Signaling Technology, 1:500), actin was used. The membranes were then washed with PBST three times and incubated with horseradish peroxidase (HRP)-conjugated secondary antibody. The Western Blots were visualized using the enhanced chemiluminescence reagents. The primary antibody was detected by an appropriate secondary antibody conjugated with horseradis peroxidase (ThermoScientific) and visualized by an ECL kit.

Transwell assay

After treating with RPMI1640, 5×10^4 cells in 400ul complete medium were inoculated in the upper chamber, coated with (invasion assay) or without (migration assay) Matrigel, and 600ul medium was added into the lower chamber. After incubation for 8 hours, cells on the upper surface of the membrane were removed by wiping with Q-tip, and the invaded cells were fixed with formaldehyde for 20 min. The cells were dyed with Giemsa staining for 20 min and redyed with Hematoxylin for 2h. The numbers of invaded and migrated cells were counted in five randomized high-power fields under a microscope.

Intravasation assay

The intravasation assay was modified as previously described [19] The first day, 1.5×10^4 human umbilical vein endothelial cells (HUVECs, Type Culture Collection of the Chinese Academy of Sciences, Shanghai, China) were sowed on the bottom side of a Transwell filter which had been pre-coated with Matrigel (1:20,BD Biosciences, Franklin Lake, NJ, USA). The cells were cultured overnight. On the second day, Hey cells were labeled with CellTracker Red CMTPX (Invitrogen Inc., Carlsbad,

CA, USA), and the endothelial cells were labeled with CellTracer Vybrant CFDA SE (Invitrogen). 5×10^4 Hey cells were seeded on the upper chamber of the Transwell filter, with RPMI 1640 medium supplemented with 1% FBS placed in the bottom chamber. Approximately

twelve hours later, all cells in the upper chamber were removed by swabbing. The cells on the lower surface were fixed with 4% paraformaldehyde. The number of intravasation tumor cells was quantified using an Olympus BX51AX-70 microscope(Olympus, Tokyo, Japan).

Extravasation assay

Similar to the intravasation assay, 5×10^4 HUVECs were seeded on the upper side of a Transwell filter that had been pre-coated with Matrigel (1:20, BD Biosciences,Franklin Lake, NJ, USA). The cells were cultured overnight. Approximately 5×10^4 Hey cells were seeded on the surface of the HUVECs, with a 1% FBS medium placed in the bottom well as a chemoattractant. After 12 hours, the tumor cells that had extravasated through the HUVECs and Matrigel on the lower surface of the Transwell were observed using microscopy.

LSCM (laser scanning confocal microscope) for observing the cytoskeleton

After treating with medium, the slides of cells were washed with PBS twice. The cells were fixed with formaldehyde for 20 min and washed with PBS three times.0.1%Triton X-100/PBS was used for 10 min, and then cells were washed with PBS three times. The cells were dyeing with FITC-Phalloidin (5ug/ml) for 30min at 37°C. After washed with PBS, the cells were stained with PI. Adding the antifade Polyvinylpyrrolidone Mounting Medium, and the cytoskeleton was observed with LSCM.

qPCR

Total RNA was extracted using the Trizol reagent (TaKaRa) according to the manufacturer's protocol. First-strand complementary DNA was synthesized using PrimeScript™ RT reagent Kit with gDNA Eraser (TaKaRa). qPCR was performed using PSYBR® Premix Ex Taq™ (TaKaRa) with CFX96TM Real-Time system(Bio-Rad) according to the manufacturer's instructions. The following primers were used: Snail, 5′-GCG AGC TGC AGG ACT CTA AT −3′ (5′-primer) and 5′- GGA CAG AGT CCC AGA TGA GC −3′ (3′- primer); Slug, 5′- CGT TTT TCC AGA CCC TGG TT −3′ (5′-primer) and 5′- CTG CAG ATG AGC CCT CAG A −3′ (3′-primer); Twist, 5′- CGC CCC GCT CTT CTC CTC T −3′ (5′-primer) and 5′- GAC TGT CCA TTT TCT CCT TCT CTG −3′ (3′-primer); Vimentin, 5′- AGA TGG CCC TTG ACA TTG AG −3′ (5′-primer) and 5′- CCA GAG GGA GTG AAT CCA GA −3′ (3′-primer); N-cadherin, 5′- CTC CTA TGA GTG GAA CAG GAA CG −3′ (5′-primer) and 5′- TTG GAT CAA TGT CAT ATT CAA GTG CTG TA −3′ (3′- Tsubaki et al. Journal of Experimental & Clinical Cancer Research 2013, 32:62 Page 2 of 9 http://www.jeccr.com/content/32/1/62primer); E-cadherin, 5′- GAA CGC ATT GCC ACA TAC AC -3′ (5′-primer) and 5′- GAA TTC GGG CTT GTT GTC AT -3′ (3′-primer);SOS1, 5′- TCCACGAAGACGACCAGAAT −3′ (5′-primer) and 5′- GGG GACTGTCCAAATGCTTA −3′(3′-primer).

As an internal control for each sample, the β-actin gene was used for standardization. Cycle threshold (Ct) values were established, and the relative difference in expression from β-actin expression was determined according to the $2^{-\Delta\Delta Ct}$ method of analysis and compared to the expression in control cells.

GST pull-down assay for Rac and Ras activation

Cell lysate from cells in the exponential growth phase was prepared. Two and 0.5 mg of lysate were used for each assay. The Rac and Ras Activation Assay Kit (Upstate, Millipore Corp., Billerica, MA, USA) were used to measure the levels of active GTP loading of Rac and Ras. Following the manufacturer's instructions, cells or tissues were lysed in ice-cold Rac and Ras activation lysis buffer and cleared with glutathione-agarose beads (Sigma, St. Louis, MO, USA). The cleared lysates were then incubated with Rac and Ras GDS RBD agarose slurry centrifuged, and washed. The agarose beads were resuspended in $2 \times$ Laemmli reducing sample buffer, boiled for 5 minutes, separated by SDS-PAGE,

and transferred to a polyvinylidene fluoride membrane (Millipore, USA). The membranes were blocked, incubated with anti-Rac and anti-Ras antibodies, and probed with HRP-conjugated secondary antibody. Immunocomplexes were visualized by chemiluminescent detection (ChemiDOC XRS; Bio-Rad, Hercules, CA, USA)

In vivo assay

Five-week-old female athymic nude mice (BALB) were intraperitoneal injection with 1×10^7 HEY cells suspended in 200 ul PBS after infection with adenovirus or not. After 5 weeks, the mice were decapitated and observed the metastasis of tumors in the abdominal cavity. All experiments using mice were reviewed by the Committee for Ethics on Animal Experiments of Chongqing Medical University.

Statistical Analysis

Statistical analysis was performed by ANOVA and the Student's t-test for continuous data. Statistical analyses were conducted using SPSS 25.0 (IBM, Armonk, NY, USA). All statistical tests were 2-sided, and $P < 0.05$ was considered to be significant.

Ethical Statement

All clinical investigations have been conducted according to the tenets of the Declaration of Helsinki. All human and animal studies have been approved by the institutional review boards and were approved for the protection of human and animal subjects in Chongqing Medical University. Written informed consent was obtained from each patient before inclusion in the study.

Results

The Expression of SOS1 was increased in EOC with high metastatic potential

To evaluate whether SOS1 expression differed in ovarian cancer cells and tissues, we assessed the expression of SOS1 in different types of tissues, including normal ovarian tissue, benign controls, and ovarian cancer tissues (Fig. 1A-B). The expression of SOS1 is higher in cancer
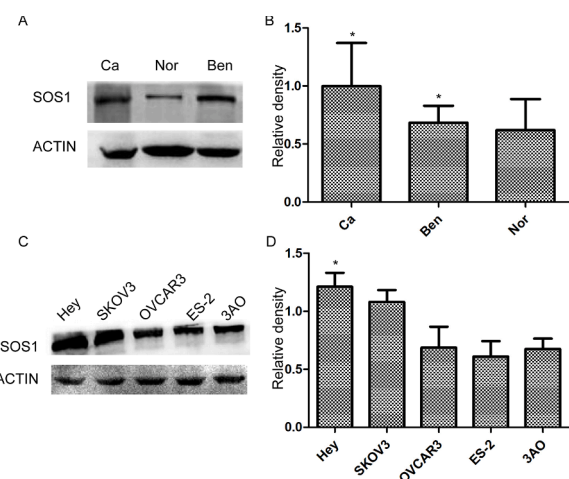
Fig. 1. SOS1 expression in epithelial ovarian cancer (EOC). (A) SOS1 expression in different types of EOC tissue. The SOS1 expression of normal, benign, and carcinoma tissue. Ca: carcinoma, Ben: benign, Nor:normal. (B) Each bar in the histogram represents the mean ± SEM of relative density (*p < 0.05). (C-D) The SOS1 expression in five ovarian cancer cell lines. The histogram indicates the expression intensity of SOS1. Four separate experimental replicates were performed.

tissues than benign and (or) normal tissues. In addition, among various ovarian cell lines, the expression of SOS1 is higher in Hey cells than other cell types ((Fig. 1C-D). The metastatic potential of Hey cells is the highest in variant ovarian cancer cell lines (Supplementary Fig. 1).

SOS1 induced the metastatic steps of EOC

To identify whether SOS1 may induce motility of EOC cells, we knocked down the expression of SOS1 in Hey and verified the expression. Empty vector-transfected cells were used as control (NT) and Hey cells were used as control (WT). Transwell assay was used to evaluate both cell migration and invasion. When knocking down SOS1 in Hey, the migration ability is decreased(272.67 ± 8.18vs.256.00 ± 2.16vs.90.00 ± 2.45, $P<0.01$) (Fig. 2A), which is consistent with the results of invasion ability(120.33 ± 2.49 vs.102.00 ± 8.94 vs.28.00 ± 1.251, $P<0.01$)

(Fig. 2B). Unlike most other cancers, ovarian carcinoma mainly disseminates through the pelvic and/or para-aortic lymph nodes, rarely through the vasculature. However, disseminates outside the abdominal cavity, such as lung and bone, might through the vasculature. To simulate the blood metastasis, we utilized matrigel gel to imitate the extracellular matrix(ECM), while HUVECs imitate the vascular wall. We exploited the intravasation and the extravasation assay to detect the ability, passing through the ECM and HUVECs of EOC cells. The process mimics blood metastasis. As we showed, the green represents the HUVECs, while the red represents the EOC cells, which migrate through the matrigel and HUVECs. Compared with Hey-NT and Hey-WT cells, the ability of Hey-SOS1i cells migrating through the matrigel and HUVEC significantly decreased(27.33 ± 3.25 vs.24.00 ± 2.16 vs.12.00 ± 1.63, $P<0.05$) (Fig. 2C). Similar to the intravasation, the extravasation indicated consistent results. Hey-SOS1i cells transferred through the
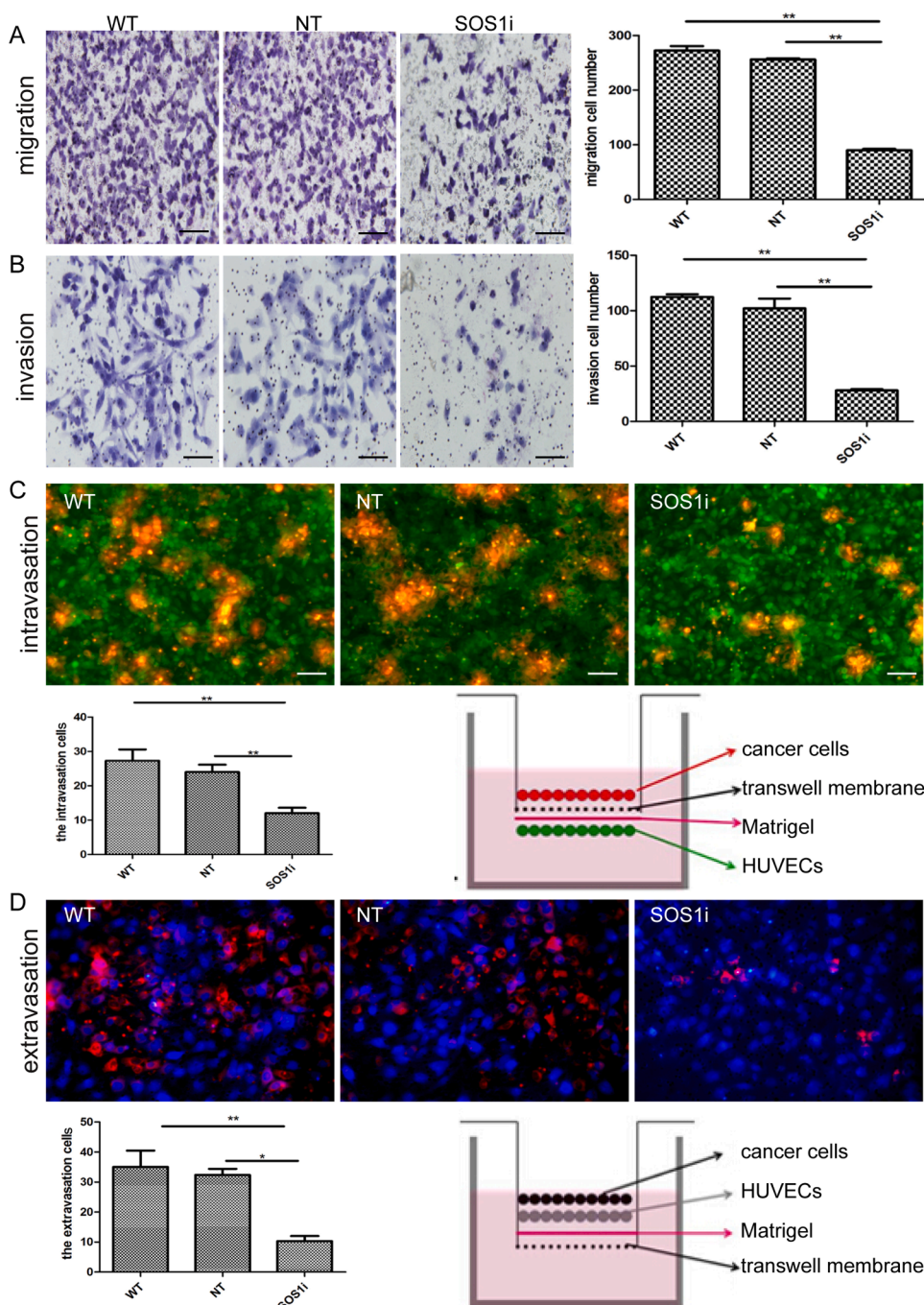
Fig. 2. In vitro experiments demonstrate the involvement of SOS1 in the metastasis of EOC. the Significantly decreased cell migration (A, upper panels), invasion through Matrigel (A, lower panels), intravasation through the basement membrane (Matrigel) and HUVECs (B), and extravasation through HUVECs and Matrigel (C) were observed in Hey cells with siRNA-mediated knockdown of SOS1 (SOS1i cells) in contrast with migration, invasion, intravasation, and extravasation of the negative controls (NT.cont). The controls bar of the histogram (right lanes) represents the mean ± SEM of three experiments, and the schematics for intravasation, and extravasation assays are given (*p < 0.05, **p < 0.01) . In the intravasation and extravasation assay, tumor cells were labeled with Cell Tracker GFP to differentiate extravasated HEY cells from HUVEC cells. Scale bars: A, B 100 μm; C 50 μm.

HUVECs and the matrigel are less than control (35.00 ± 5.47vs.32.34 ± 2.06 vs.10.33 ± 1.67, $P<0.05$) (Fig. 2D). These results indicated that depletions of SOS1 could reduce the metastatic ability of Hey cells.

Knockdown of SOS1 reversed the EMT process

The phalloidin was used to label the actin cytoskeleton of Hey cells to observe the effect of SOS1 silencing on a cellular skeleton and cellular pseudopods. The myofilament of the cellular skeleton became sparse and cellular pseudopod reduced while the connection between cells became tight(Fig. 3A). These data suggested that SOS1 silencing could change the morphology of Hey cells, These changes indicated that the cells changed from stromal to epithelioid, suggesting that the migration ability of cells was weakened.

Hence, we investigated whether the markers of EMT process were changed after knocking down SOS1. As the qPCR and Western Blot showed, the expression of epithelial marker E-cadherin was increased, while mesenchymal markers N-cadherin and Vimentin decreased. Meanwhile, the expression of MMP2 and MMP9, the significant protein of EMT, was also declined (Fig. 3B-D). EMT promoting transcription factors, such as twist, snail, and ZEB family, have crucial effects in EMT process. We evaluated their expression to identify the reverse effect on EMT. The mRNA and protein expression of snail is decreased, whereas the level of twist and slug has no change when knockdown SOS1(Fig. 3B-D). These results indicated that SOS1 plays a vital role in the EMT process in Hey cells, which promotes the metastatic potential of Hey cells.

SOS1 increased the activation of NF-κB

To investigate which signaling pathways are activated when SOS1 induces EMT in Hey cells, we examined the changes that occur in NF-κB, Ras-ERK/JNK/P38, Wnt, and PI3K-AKT signaling pathway. As shown in
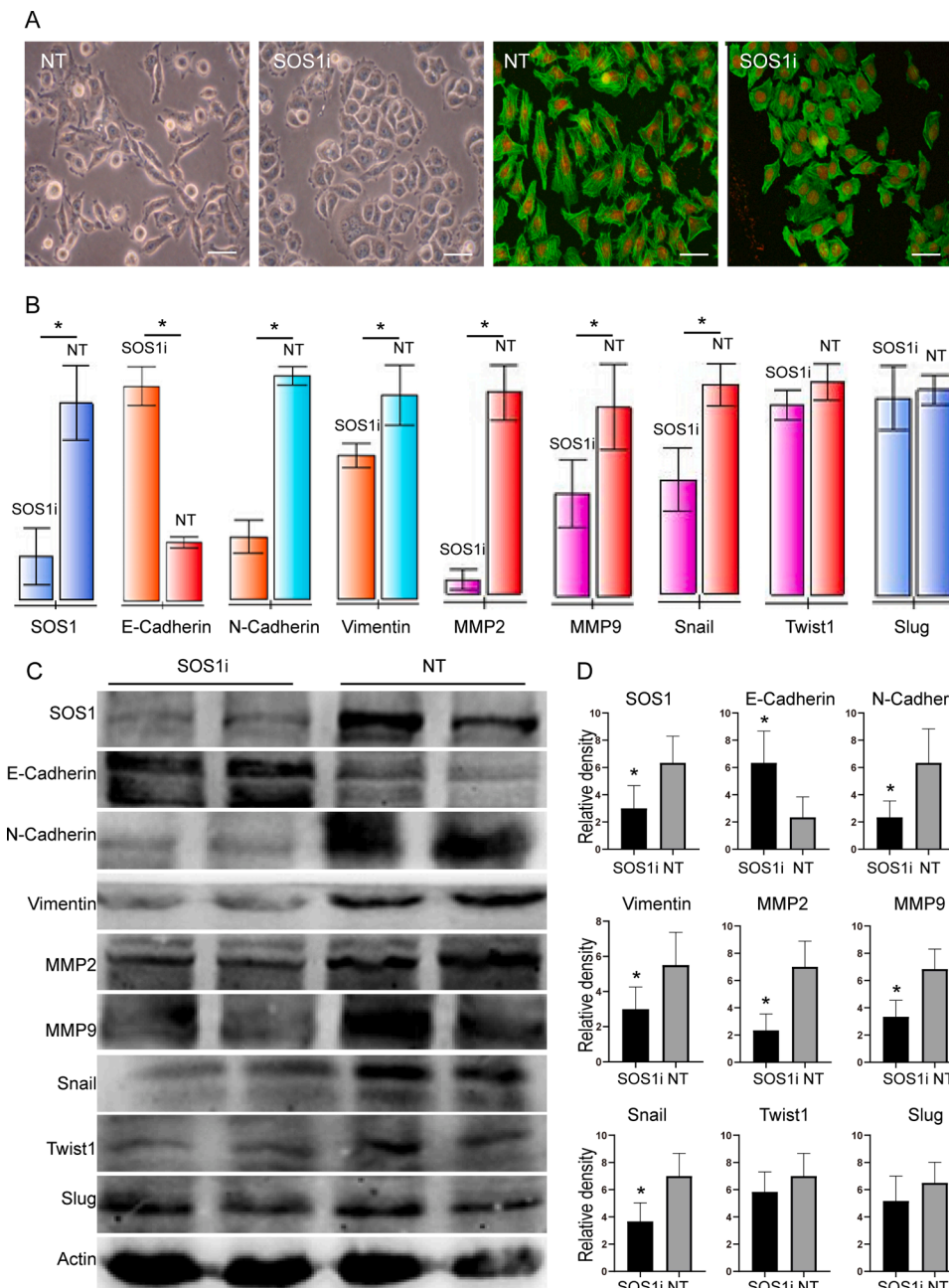
Fig. 3. The effect of SOS1 on the EMT of Hey cells. (A) Hey cells cellular morphology, skeleton and cellular pseudopods were observed (*400); (B)The mRNA expression of SOS1, N-cadherin, Vimentin, MMP9, MMP2 and Snail are reduced in Hey cells, but the mRNA expression of E-cadherin is increased. Each bar in the histogram represents the mean ± SEM of relative OD values (*p < 0.05); (C) A similar trend of the protein expression was detected. Each bar in the histogram represents the mean ± SEM of relative OD values (*p < 0.05). Four separate experimental replicates were performed. Scale bars: A 100 μm.

A

B

C

D

E

F
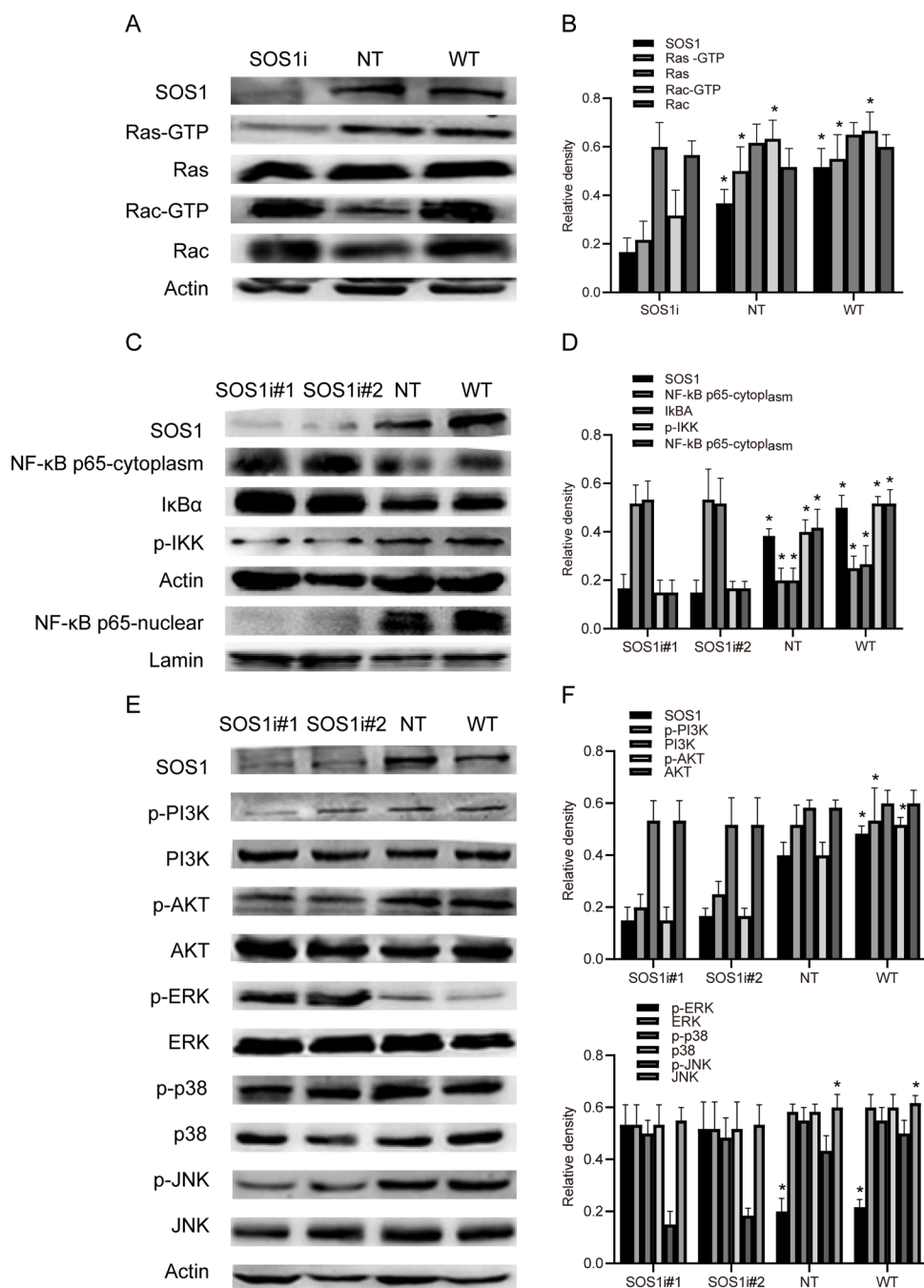
Fig. 4. Knockdown of SOS1 inhibits the activation of NF-κB pathway. (A-B) Rac-GTP and Ras-GTP were detected in SOS1i cells by using a GST-pull down assay. A reduced Ras-GTP level was detected in SOS1i cells, but not detected in the Rac-GTP level. (C-D) Knockdown of SOS1 suppresses Ras-ERK/P38MAPK/JNK pathway. (E-F) Knockdown of SOS1 inhibits NF-κB pathway. Each bar represents the mean ± SEM of relative OD values (*p < 0.05). Four separate experimental replicates were performed.

Fig. 4, only NF-κB and PI3K-AKT signaling pathways changed in accordance with the above experimental results(Fig. 4A, B, E, F). Silencing SOS1 not only up-regulated the expression of cytoplasmic NF-κB p65 but also inhibited the active NF-κB p65 in nucleus (Fig. 4C, D). In addition, silencing SOS1 reduced the phosphorylated PI3K and AKT levels, while the protein expression of Bcl-2 and Bax, the two major downstream target genes, did not change significantly. Unexpectedly, ERK activity increased after silencing SOS1 expression in our study, and the specific mechanism needs to be further studied.

As IκBα binds to NF-κB preventing its transfer to the nucleus, the degradation of IκBα releases NF-κB p65 to the nucleus. Then we measured the IκBα cytoplasm levels and found that statistically significantly decreased IκBα degradation in SOS1i cells (Fig. 4C, D). We utilized Western blot to investigate IKKα phosphorylation to decide if the IκBα degradation inhibition is an outcome of IKKα phosphorylation

inhibition. Knocking down SOS1 appreciably reduced the levels of phosphorylated IKKα in cytoplasm (Fig. 4C, D). These outcomes reveal that SOS1 aid nuclear stimulation of NF-κB probably by promoting IκBα degradation via increasing the level of phosphorylated IKKα.

Overexpression of SOS1 improved malignant potential and induce the EMT through AKT-independent NF-κB activation

To further explore the biological effect of SOS1, SOS1 was stably transfected into OVCAR3 cells (overexpression of SOS1, ADSOS1). Empty vector-transfected cells were used as control (NT) and Hey cells were used as control (WT). Ectopic overexpression SOS1 was determined by RT-PCR and Western Blot (Fig. 5B, C). SOS1 overexpression markedly increased OVCAR3 migration and invasion in vitro (Fig. 5A). The expression levels of the transcriptional repressors of N-cadherin,
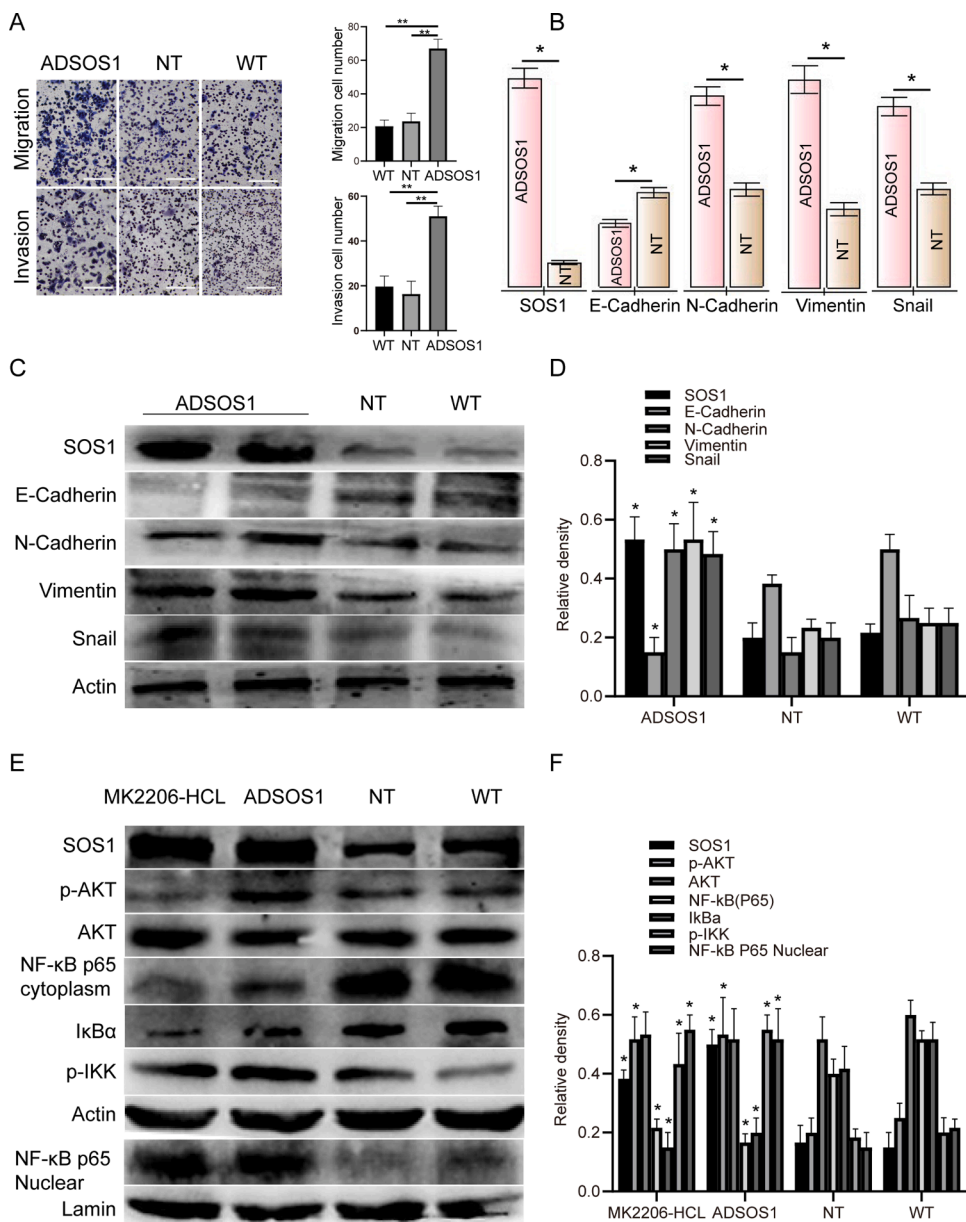
Fig. 5. SOS1 increases Snail expression and induces EMT through AKT-independent NF-κB activation. (A) Overexpression of SOS1 promotes migration and invasion of OVCAR3 cells. (B) Overexpression of SOS1 induces the mRNA level of N-cadherin, Vimentin and Snail in OVCAR3 cells, but reduces that of E-cadherin. (C) A similar trend of the protein expression was detected. (D) The inhibitor of p-AKT, MK2206-HCL, inhibits the activation of p-AKT, but could not influence the NF-κB pathway. Each bar in the histogram represents the mean ± SEM of relative OD values (*p < 0.05, **p < 0.01). Four separate experimental replicates were performed. Scale bars: A 50 μm.

vimentin, and Snail were upregulated in SOS1-overexpression OVCAR3 cells (Fig. 5B, 5C), but that of N-cadherin reduced. Next, we investigated whether SOS1 overexpression could activate PI3K-AKT and NF-κB signaling pathways. In ADSOS1 OVCAR3 cells, NF-κB p65 in nucleus expression increased significantly, Meanwhile, these in cytoplasm decreased. When engaging MK2206-HCL (Boston, 3 μM dose) for 48h, an inhibitor of p-AKT, the expression of p-AKT decreased significantly, whereas the NF-κB p65 has not significantly changed. These indicate SOS1 promotes EMT through AKT independent NF-κB signaling in OVCAR3 cells.

SOS1 gave rise to the intraperitoneal metastasis in vivo

The majority of EOC patients present at an advanced stage, with the widely spread metastatic disease within the peritoneal cavity [20]. To further verify the oncogenic role of SOS1, we established the mice tumor model using the Hey-NT and Hey-SOS1i cells to mimic intraperitoneal metastasis (Fig. 6C). As shown in Fig. 6A and B and Table 1, SOS1 silencing resulted in a smaller cloud of lesions and limited metastasis, compared with the NT.cont group. The number of tumor nodules in the

peritoneal cavity was reduced (2-fold) in the SOS1i group. In bowel and mesentery, the metastasis nodules were significantly reduced between the above two groups. However, in the liver and stomach, the metastasis nodules exhibited no statistical difference. These results confirmed that knocking down SOS1 could inhibit EOC cells metastasis in vivo, that is to say, our results indicated that SOS1 plays an essential role in abdominal cavity metastasis of EOC.

Discussion

In the present study, we showed that SOS1 played a vital role in cell migration and invasion. Combined with these current results, SOS1 may be involved in the regulation of cell motility by following mechanisms, SOS1 could be used as GEFs of Rac, or via forming a complex with EPS8/ABL1 to activate Rac. The activated Rac regulates the cytoskeleton through JNK signaling pathway, which could regulate cell movement subsequently [13]. In recent years, the role of EMT in tumor progression has been gradually recognized. Sarmishtha de et al. found that EGFR activates NF-κB by SOS1, which is independent of the guanine nucleotide exchange activity of SOS1 [12]. Nucleus-located NF-κB promotes
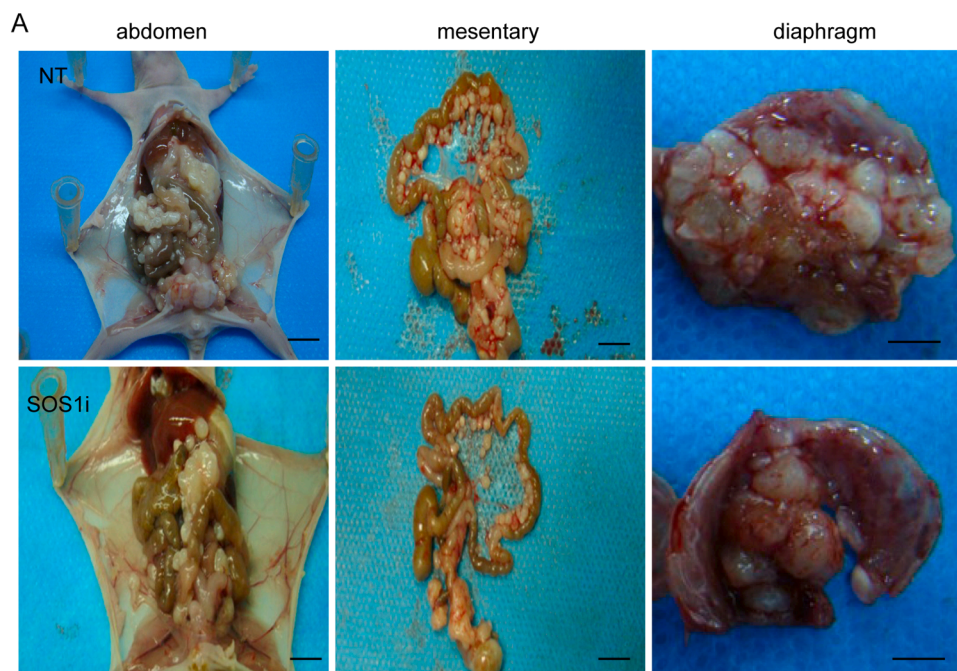
Fig. 6. . The metastasis intraperitoneal in nude mice. Hey cells (SOS1i or NT.cont) were injected into the peritoneal cavity of nude mice. Five weeks later, mice were euthanized and analyzed: all mice in the groups had tumors within the peritoneal cavity. (A) Metastatic foci in the abdomen, mesentery and diaphragm are shown. Decreased metastatic lesions were detected within abdomen, especially in the mesentery and diaphragm in the SOS1i group. (B) The number of metastatic lesions in the abdominal cavity of the two groups, according to the target organ, (*$p < 0.05$, **$p < 0.01$). (C) SOS1 expression was detected in the implants from the abdomen of mice in the NT.cont and SOS1i groups, (*$p < 0.05$). Three separate experimental replicates were performed. Scale bars: A 50 mm.
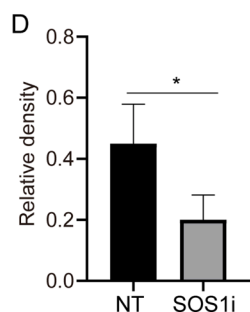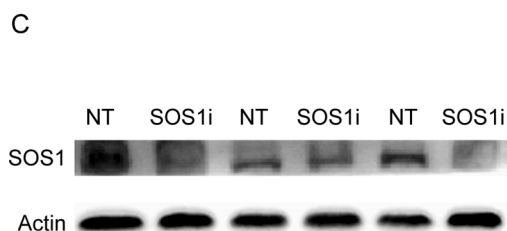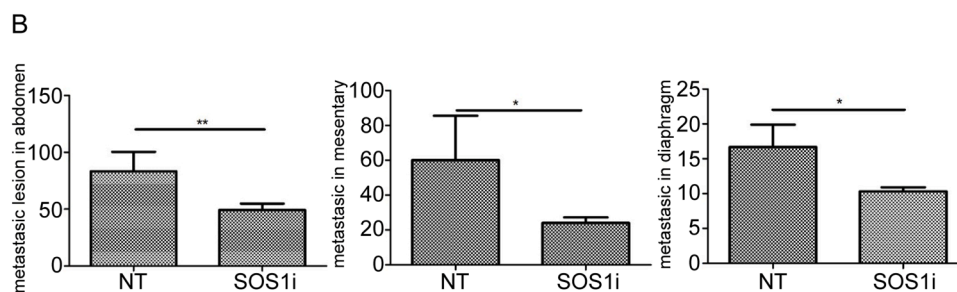
Table 1

: Implantation of abdominal and pelvic organs in intraperitoneal models in nude mice.

	The implantation of organs		Implantation numbers (>1mm^3)	
groups	NT(n=3)	SOS1i)n=3(	NT(n=3)	SOS1i)n=3(
weight)g(	28.76	27.79	28.76	27.79
Intestine	3/3	3/3	58.67±10.53	33±4.32*
liver	1/3	1/3	6.67±1.45	6.00±1.67
Liver capsular	3/3	3/3	10.67±2.87	6.00±3.74
stomach	3/3	3/3	2.00±1.00	1.67±0.58
diaphragm	3/3	3/3	16.67±3.21	10.33±0.58*
Renal capsular	3/3	2/3	5.00±0.13	3.33±1.53
Renal paraenhyma	0/3	0/3		
peritoneum	3/3	3/3	15.00±6.37	6.00±0.81*

* $p < 0.05$

the transcription of snail, which directly acts upon the E-box region of E-cadherin to inhibit the expression of E-cadherin, promotes the occurrence of EMT, and enhances the migration and invasion ability of cells [21].

In this experiment, after knocking down SOS1 expression, the fibroblast-like morphology of cells was reversed; the arrangement of cytoskeleton myofilaments was disordered and sparsed; the cell protruding was markedly reduced, and the intercellular arrangement was tight. Meanwhile, the migration and invasion ability of cells was decreased. The cell events caused by Rac/JNK signaling pathway are isolated and single [22], so it is difficult to systematically and comprehensively explain the series of the above results. However, EMT is a dynamic and adjustable process, the increased expression of E-cadherin may induce the above morphological changes and cell events by inhibiting and reversing the EMT process.

The results of in vitro experiments showed that the invasion ability of

Hey cells was significantly impaired after the expression of SOS1 was interfered. To verify the above results in vivo, we successfully established an intraperitoneal implantation model in immunodeficient mice using SOS1i cells. Five weeks after implantation, the carcinoma focus showed extensive metastasis in the pelvic and abdominal organs of nude mice, such as omentum and peritoneum. Clinically, the most easily metastatic sites of ovarian cancer are greater omentum and pelvic peritoneum, which are similar to the clinical phenotype of patients with ovarian cancer. When the expression of SOS1 was down-regulated, the total number of metastatic lesions in abdominal visceral organs of nude mice decreased. The number of metastatic lesions in intestinal, mesenteric, and diaphragmatic organs was significantly different, while the metastasis of other organs such as omentum, liver and spleen has not markedly changed. It is suggested that SOS1 may play an important role in the regulation of visceral metastasis of ovarian cancer. But in our experiment, there was no significant difference in the order of organ involvement between the two groups. The reasons may be as follows, on the one hand, without fully considering the transfer abilities of the cells, we reared the nude mice for a long time after the cells were planted, which may lead to extensive intraperitoneal metastasis. On the other, the adhesion experiment in vitro suggested that the down-regulation of SOS1 expression reduced cell adhesion, which may be one of the reasons for the decrease of intestinal metastasis.

SOS1 activates a variety of downstream pathways via forming functional trimers. SOS1 induces the activation of NF-κB mediated by the I-κB kinase complex [10, 21]. Members of the mitogen-activated protein kinase family, including JNK and ERK, are activated downstream of SOS1 [23, 24]. SOS1 also induces the activation of the phosphoinositol 3-kinase/Akt/mTOR pathway [25, 26]. The present study has demonstrated that SOS1 induced activation of NF-κB, but not of ERK1/2, AKT, JNK, and STAT3. Sarmishtha de et al. found that EGFR can activate NF-κB by using SOS1, which is independent of the guanine nucleotide exchange activity of SOS1 [10]. Moreover, in the over-expression SOS1 EOC cells, MK2022-HCL [27], a p-AKT inhibitor, did not inhibit SOS1-induced p-IKKα and increased the IκBα expression. Our results also indicate that SOS1 increases the activation of NF-κB and the expression of Snail through AKT-independent NF-κB activation, which is consistent with Sarmishtha de's findings. Therefore, we speculate that SOS1 induces the EMT in epithelial ovarian cancer(EOC) cells with high metastatic potential via AKT-independent NF-κB signing pathway, which is independent of the guanine nucleotide exchange activity of SOS1.

The present study has a lot of limitations. The clinical cases in this research were limited and all cases were from a single center. Moreover, the study on the pathway of AKT independent NF-κB signaling is not comprehensive and more thorough pathway studies are needed to clarify the mechanism.

In summary, the present study has found that SOS1 promotes the invasion, intravasation, extravasation, and metastasis of EOC cells. SOS1 also induces EMT through AKT independent NF-κB signaling. That is to say, SOS1 may play a pivotal role in the metastasis of EOC cells, which might become a novel treatment target of EOC, especially of those with high metastatic potential.

Declaration of Competing Interest

The authors declare that they have no conflict of interest.

Authors contributions

Conceptualization: Feiji Sun.
Methodology: Min Cheng, Xiaolin Ye, Jiemin Dai.
Software: Min Cheng, Xiaolin Ye.
Validation: Min Cheng, Xiaolin Ye.
Formal analysis: Min Cheng, Jiemin Dai.
Investigation: Min Cheng, Xiaolin Ye.

Resources: Feiji Sun, Min Cheng.
Data curation: Feiji Sun, Min Cheng.
Writing (original draft preparation): Min Cheng.
Writing (review and editing): Feiji Sun, Min Cheng.
Visualization: Feiji Sun, Min Cheng.
Supervision: Feiji Sun.

Supplementary materials

Supplementary material associated with this article can be found, in the online version, at doi:10.1016/j.tranon.2021.101160.

Reference

[1] R.L. Siegel, K.D. Miller, A.o.t. Jemal, Cancer statistics, 2019, CA Cancer J Clin 69 (2019) 7–34.

[2] M. Shih Ie, R.J. Kurman, Ovarian tumorigenesis: a proposed model based on morphological and molecular genetic analysis, Am J Pathol 164 (2004) 1511–1518.

[3] A.F. Chambers, A.C. Groom, I.C. MacDonald, Dissemination and growth of cancer cells in metastatic sites, Nat Rev Cancer 2 (2002) 563–572.

[4] E. Korsching, J. Packeisen, C. Liedtke, D. Hungermann, P. Wulfing, P.J. van Diest, B. Brandt, W. Boecker, H. Buerger, The origin of vimentin expression in invasive breast cancer: epithelial-mesenchymal transition, myoepithelial histogenesis or histogenesis from progenitor cells with bilinear differentiation potential? J Pathol 206 (2005) 451–457.

[5] Y. Kanegae, A.T. Tavares, J.C. Izpisua Belmonte, I.M. Verma, Role of Rel/NF-kappaB transcription factors during the outgrowth of the vertebrate limb, Nature 392 (1998) 611–614.

[6] T. Bogenrieder, M. Herlyn, Axis of evil: molecular mechanisms of cancer metastasis, Oncogene 22 (2003) 6524–6536.

[7] A. Hall, Rho GTPases and the actin cytoskeleton, Science 279 (1998) 509–514.

[8] J.L. Bos, Linking Rap to cell adhesion, Curr Opin Cell Biol 17 (2005) 123–128.

[9] A.L. Knox, N.H. Brown, Rap1 GTPase regulation of adherens junction positioning and cell adhesion, Science 295 (2002) 1285–1288.

[10] B. De Craene, G. Berx, Regulatory networks defining EMT during cancer initiation and progression, Nat Rev Cancer 13 (2013) 97–110.

[11] N. Zarich, J.L. Oliva, N. Martinez, R. Jorge, A. Ballester, S. Gutierrez-Eisman, S. Garcia-Vargas, J.M. Rojas, Grb2 is a negative modulator of the intrinsic Ras-GEF activity of hSos1, Mol Biol Cell 17 (2006) 3591–3597.

[12] S. De, J.K. Dermawan, G.R. Stark, EGF receptor uses SOS1 to drive constitutive activation of NFkappaB in cancer cells, Proc Natl Acad Sci U S A, 111 (2014) 11721–11726.

[13] H. Chen, X. Wu, Z.K. Pan, S. Huang, Integrity of SOS1/EPS8/ABI1 tri-complex determines ovarian cancer metastasis, Cancer Res 70 (2010) 9979–9990.

[14] M.A. Nieto, The snail superfamily of zinc-finger transcription factors, Nat Rev Mol Cell Biol 3 (2002) 155–166.

[15] J. Comijn, G. Berx, P. Vermassen, K. Verschueren, L. van Grunsven, E. Bruyneel, M. Mareel, D. Huylebroeck, F. van Roy, The two-handed E box binding zinc finger protein SIP1 downregulates E-cadherin and induces invasion, Mol Cell 7 (2001) 1267–1278.

[16] A. Eger, K. Aigner, S. Sonderegger, B. Dampier, S. Oehler, M. Schreiber, G. Berx, A. Cano, H. Beug, R. Foisner, DeltaEF1 is a transcriptional repressor of E-cadherin and regulates epithelial plasticity in breast cancer cells, Oncogene 24 (2005) 2375–2385.

[17] M. Perrais, X. Chen, M. Perez-Moreno, B.M. Gumbiner, E-cadherin homophilic ligation inhibits cell growth and epidermal growth factor receptor signaling independently of other cell interactions, Mol Biol Cell 18 (2007) 2013–2025.

[18] J. Su, S.M. Morgani, C.J. David, Q. Wang, E.E. Er, Y.H. Huang, H. Basnet, Y. Zou, W. Shu, R.K. Soni, R.C. Hendrickson, A.K. Hadjantonakis, J. Massague, TGF-beta orchestrates fibrogenic and developmental EMTs via the RAS effector RREB1, Nature 577 (2020) 566–571.

[19] N.E. Ramirez, Z. Zhang, A. Madamanchi, K.L. Boyd, L.D. O'Rear, A. Nashabi, Z. Li, W.D. Dupont, A. Zijlstra, M.M. Zutter, The alpha(2)beta(1) integrin is a metastasis suppressor in mouse models and human cancer, J Clin Invest 121 (2011) 226–237.

[20] M. Tsuda, S. Tanaka, Roles for crk in cancer metastasis and invasion, Genes Cancer 3 (2012) 334–340.

[21] A. Cano, M.A. Perez-Moreno, I. Rodrigo, A. Locascio, M.J. Blanco, M.G. del Barrio, F. Portillo, M.A. Nieto, The transcription factor snail controls epithelial-mesenchymal transitions by repressing E-cadherin expression, Nat Cell Biol 2 (2000) 76–83.

[22] C. Weston, C. Gordon, G. Teressa, E. Hod, X.D. Ren, J. Prives, Cooperative regulation by Rac and Rho of agrin-induced acetylcholine receptor clustering in muscle cells, J Biol Chem 278 (2003) 6450–6455.

[23] M.A. Lomaga, W.C. Yeh, I. Sarosi, G.S. Duncan, C. Furlonger, A. Ho, S. Morony, C. Capparelli, G. Van, S. Kaufman, A. van der Heiden, A. Itie, A. Wakeham, W. Khoo, T. Sasaki, Z. Cao, J.M. Penninger, C.J. Paige, D.L. Lacey, C.R. Dunstan, W. J. Boyle, D.V. Goeddel, T.W. Mak, TRAF6 deficiency results in osteopetrosis and defective interleukin-1, CD40, and LPS signaling, Genes Dev 13 (1999) 1015–1024.

[24] A.P. Armstrong, M.E. Tometsko, M. Glaccum, C.L. Sutherland, D. Cosman, W. C. Dougall, A RANK/TRAF6-dependent signal transduction pathway is essential for osteoclast cytoskeletal organization and resorptive function, J Biol Chem 277 (2002) 44347–44356.

[25] D.K. Morrison, MAP kinase pathways, Cold Spring Harb Perspect Biol (2012) 4.

[26] T. Wada, J.M. Penninger, Mitogen-activated protein kinases in apoptosis regulation, Oncogene 23 (2004) 2838–2849.

[27] N. Koundouros, E. Karali, A. Tripp, A. Valle, P. Inglese, N.J.S. Perry, D.J. Magee, S. Anjomani Virmouni, G.A. Elder, A.L. Tyson, M.L. Doria, A. van Weverwijk, R. F. Soares, C.M. Isacke, J.K. Nicholson, R.C. Glen, Z. Takats, G. Poulogiannis, Metabolic Fingerprinting Links Oncogenic PIK3CA with Enhanced Arachidonic Acid-Derived Eicosanoids, Cell 181 (2020) 1596–1611, e1527.